

## *Rapid Publication*

# Candidate Loci for Zimmermann–Laband Syndrome at 3p14.3

**Hyung-Goo Kim,<sup>1</sup> Anne W. Higgins,<sup>2</sup> Steven R. Herrick,<sup>2</sup> Shotaro Kishikawa,<sup>1</sup> Linda Nicholson,<sup>3</sup> Kerstin Kutsche,<sup>4</sup> Azra H. Ligon,<sup>2</sup> David J. Harris,<sup>5</sup> Marcy E. MacDonald,<sup>6</sup> Gail A.P. Bruns,<sup>5</sup> Cynthia C. Morton,<sup>7</sup> Bradley J. Quade,<sup>2</sup> and James F. Gusella<sup>1\*</sup>**

<sup>1</sup>Molecular Neurogenetics Unit, Center for Human Genetic Research, Massachusetts General Hospital/Department of Genetics, Harvard Medical School, Boston, Massachusetts  
<sup>2</sup>Department of Pathology, Brigham and Women's Hospital/Harvard Medical School, Boston, Massachusetts  
<sup>3</sup>Nemours Children's Clinic, Alfred I. Dupont Hospital for Children, Wilmington, Delaware  
<sup>4</sup>Institut für Humangenetik, Universitätsklinikum Hamburg-Eppendorf, Hamburg, Germany  
<sup>5</sup>Division of Genetics, The Children's Hospital/Harvard Medical School, Boston, Massachusetts  
<sup>6</sup>Molecular Neurogenetics Unit, Center for Human Genetic Research, Massachusetts General Hospital/Department of Neurology, Harvard Medical School, Boston, Massachusetts  
<sup>7</sup>Departments of Obstetrics, Gynecology and Reproductive Biology and Pathology, Brigham and Women's Hospital/Harvard Medical School, Boston, Massachusetts

Received 21 July 2006; Accepted 27 September 2006

A male with 46,XY,t(3;17)(p14.3;q24.3) presented with gingival hyperplasia, hypertrichosis, unusually large ears and marked hypertrophy of the nose, characteristic of the Zimmermann–Laband syndrome (ZLS). Other features include large facial bones and mandibles, large protruding upper lip, enlarged fingers and toes, strabismus, and enlarged phallus. Knowledge of a 46,XX,t(3;8)(p21.2;q24.3) reported previously in a mother and daughter with ZLS suggests that the 3p14.3-p21.2 region may contain a gene responsible for ZLS. We have reassessed the chromosome 3 breakpoint region of the t(3;8) and revised its breakpoint location to 3p14.3, based upon an updated human genome sequence assembly. Using fluorescence in situ hybridization (FISH) with BAC clones, we have also identified a breakpoint

spanning clone at 3p14.3 in our t(3;17) patient, thereby narrowing the breakpoint to a region of approximately 200 kb. These data suggest that the gene responsible for ZLS is located in 3p14.3 and implicates four likely candidate genes in this region: *CACNA2D3*, encoding a voltage-dependent calcium channel, *LRTM1*, a gene of unknown function embedded within *CACNA2D3*, *WNT5A*, encoding a secreted signaling protein of the WNT family, and *ERC2*, which codes for a synapse protein. © 2006 Wiley-Liss, Inc.

**Key words:** Zimmermann–Laband syndrome; chromosome translocation; gingival hyperplasia; hypertrichosis; unusual facies; *CACNA2D3*; *LRTM1*; *WNT5A*; *ERC2*

**How to cite this article:** Kim H-G, Higgins AW, Herrick SR, Kishikawa S, Nicholson L, Kutsche K, Ligon AH, Harris DJ, MacDonald ME, Bruns GAP, Morton CC, Quade BJ, Gusella JF. 2007. Candidate loci for Zimmermann–Laband syndrome at 3p14.3. *Am J Med Genet Part A* 143A:107–111.

### INTRODUCTION

Zimmermann–Laband syndrome (ZLS) (MIM 135500) is a rare inherited disorder characterized by gingival fibromatosis, hypertrichosis, skeletal and soft tissue abnormalities including bulbous soft nose, thickened lips, thick and floppy ears, and aplasia or dysplasia of the nails. In addition, hepatosplenomegaly [Pfeiffer et al., 1992; Robertson et al., 1998] and mental retardation [Zimmermann, 1928; Oikawa et al., 1979; Chodirker et al., 1986; de Pina Neto et al., 1988; Il'ina et al., 1988; Bazopoulou-Kyrkani-dou et al., 1990; Pfeiffer et al., 1992; Van Buggenhout

et al., 1995] were observed in some patients. Since Zimmermann published the first two patients in 1928

Grant sponsor: USPHS; Grant numbers: GM061354, HD28138; Grant sponsor: Deutsche Forschungsgemeinschaft; Grant numbers: KU 1240/3-1, KU 1240/3-2.

\*Correspondence to: James F. Gusella, Ph.D., Molecular Neurogenetics Unit, Center for Human Genetic Research, Massachusetts General Hospital, 185 Cambridge St., Boston MA 02114.

E-mail: gusella@helix.mgh.harvard.edu

DOI 10.1002/ajmg.a.31544

[Zimmermann, 1928], a total of 39 patients with ZLS have been reported worldwide [Holzhausen et al., 2003; Stefanova et al., 2003; Shah et al., 2004; Atabek et al., 2005; Davalos et al., 2005]. Autosomal dominant inheritance has been suggested [Laband et al., 1964; Alavandar, 1965], but the molecular mechanism has not yet been elucidated. A balanced familial 3;8 chromosomal translocation that segregates with the ZLS phenotype has suggested a disease gene locus either at 3p21.2 or 8q24.3, where a disease gene might be disrupted at either of the translocation breakpoints [Stefanova et al., 2003]. Here, we report on another chromosomal anomaly associated with ZLS, an apparently balanced reciprocal translocation:  $t(3;17)(p14.3;q24.3)$ . We have designated this patient DGAP003 and investigated the breakpoints using a fibroblast cell line as part of the Developmental Genome Anatomy Project (DGAP). This work was carried out with prior review and approval by the Partners HealthCare Institutional Review Board. DGAP aims to identify genes of importance in development at or near the breakpoints of apparently balanced chromosome rearrangements associated with developmental phenotypes. We also reassessed the previously reported  $t(3;8)$  patient and repositioned the breakpoint to 3p14.3, comparable to that of DGAP003 patient. Consequently, we hypothesize that the gene responsible for ZLS is located at 3p14.3 and we report FISH analyses to refine the breakpoint region and to identify positional candidate genes for ZLS therein.

## MATERIALS AND METHODS

### Clinical Report

The patient, a black male, first came to medical attention due to absence of tooth eruption at 18 months of age. Physical examination revealed gingival hyperplasia. In addition, the subject had excess facial, body, and pubic hair. An enlarged penis was noted, along with moderately sized immature testicles bilaterally, unusually large muscles of the upper and lower limbs, as well as enlarged fingers and toes. Strabismus was also present. The patient was seen again at almost 3 years of age and was found to have distinctive facies with large facial bones and mandibles, large ears, a markedly enlarged nose with short columella and low nasal bridge. Figure 1 illustrates phenotypes displayed by the subject at 3.5 years of age, when a biopsy of the gingiva demonstrated marked epithelial thickening, and chronic inflammation and fibrosis of the underlying connective tissue. At this time, the patient was found to carry an apparently balanced chromosome rearrangement with a  $46,XY,t(3;17)(p14.3;q24.3)dn$  karyotype, which was not detected in his parents (Fig. 2). At 3.5 years of age, the patient had speech articulation problems due to gingival hypertrophy,

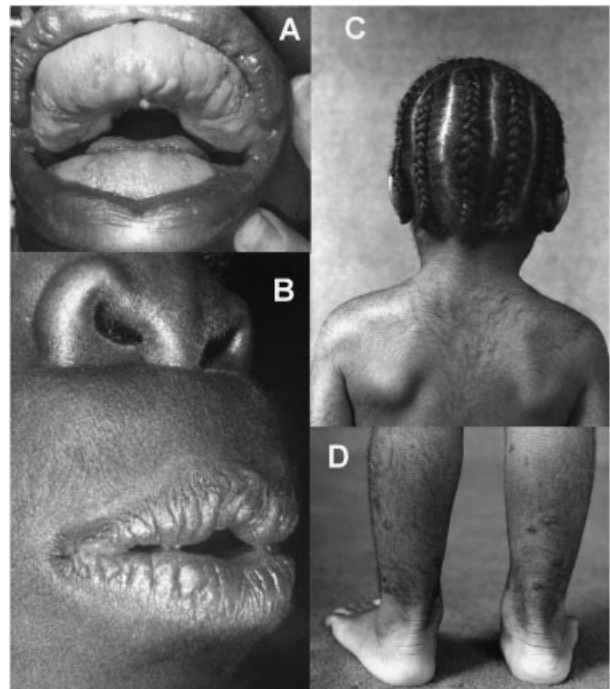


FIG. 1. ZLS phenotypes displayed by DGAP003 at 3.5 years of age. **A:** View of the partially opened mouth demonstrating marked hyperplasia of the gingivae of both dental arches; **B:** Partial view of the face showing the wide nose with a short columella, and a prominent, smooth philtrum; **C:** Posterior view showing low scalp hairline and excessive hair on the back; **D:** Posterior view of the hypertrichosis of the lower extremities.

although speech development and intelligence were normal. Physical examination revealed hypertelorism with bilateral convergent strabismus, epicanthal folds, depressed nasal bridge, large nose, protruding

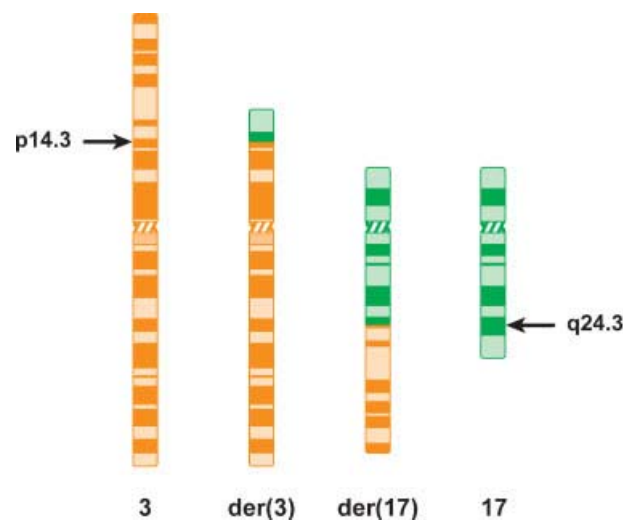


FIG. 2. Ideogram illustrating the apparently balanced chromosome  $t(3;17)(p14.3;q24.3)$  in DGAP003. A portion of the short arm of chromosome 3 was exchanged with a portion of the long arm of chromosome 17, resulting in  $der(3)$  and  $der(17)$ , respectively. At this level of resolution provided by standard GTG-banding, the translocation appeared balanced (not shown). Black arrows indicate the locations of breakpoints.

upper lip, and hypertrophic papillae on the posterior of the tongue, bilateral spade-like fingers and skin thickening on the legs. Throughout childhood, this patient underwent multiple gingivectomies. At 10 years of age, a skeletal survey revealed broad tufts of the fingers, slightly bulbous soft tissue of the fingertips, and undermodeling of the diaphyses of the phalanges and metacarpals, making these bones tubular in configuration. The metacarpals were short relative to the phalanges, while the diaphyses of the long bones were slightly undermodeled. There was widening of the shafts of the tibiae and the ribs. A craniofacial disproportion with prominence of the mandible was noted and the maxillary spine and maxillary incisors were absent. Several dysmorphic skeletal features were primarily related to undermodeling of the diaphyses of the bones.

### Cytogenetic and Fish Studies

A fibroblast cell line (GM02963) from patient DGAP003, with the reported karyotype 46,XY,t(3;17)(p14.3;q24.3)dn, was obtained from the NIGMS Human Genetic Cell Repository. Bacterial artificial chromosome (BAC) clones were obtained from CITB-D and RP11 libraries (Invitrogen, San Diego, CA and the Children's Hospital of Oakland Research Institute, Oakland, CA) and directly labeled with Spectrum Orange or Green-dUTP (Vysis) by nick translation. Hybridizations were carried out according to manufacturers' protocols. Metaphase chromosomes were counterstained with 4,6-diamino-2-phenylindole-dihydrochloride (DAPI), and at least 10 metaphases were analyzed using a Zeiss Axioskop microscope. Images were captured with a CytoVision system (Applied Imaging, San José, CA).

### RESULTS AND DISCUSSION

Of a total of 39 ZLS patients reported, transmission of a balanced chromosomal aberration, t(3;8)(p21.2;q24.3)mat, has been described once in mother and daughter [Stefanova et al., 2003]. The patient presented here offered the potential to facilitate positional cloning of the ZLS gene, because sufficient familial patients for linkage analysis are not available. Stefanova et al. [2003] mapped the breakpoint on der(3) between two breakpoint-flanking BAC clones, RP11-680P23 and RP11-189K9, defining a putative breakpoint region of 1.5 Mb in 3p21.2. We have reassessed these data in more recent human genome assemblies, including the March 2006 assembly as implemented in the Human Genome Browser (<http://genome.ucsc.edu/cgi-bin/hgGateway>). The chromosome 3 breakpoint region defined by these two clones is now reported to encompass approximately 3.2 Mb located in 3p14.3, and not 3p21.2 as previously suggested.

The phenotype of DGAP003, the male subject that we describe here, includes gingival hyperplasia, hypertrichosis, enlarged nose, large ears, unusual facies, large protruding upper lip, and bulbous soft tissues of the fingertips. Collectively, these features are most suggestive of ZLS and are comparable to the familial ZLS patients associated with the t(3;8) [Stefanova et al., 2003]. DGAP003 also exhibited problems with speech articulation that are likely due to gingival hypertrophy. The observation of overgrown gingival tissues affecting the ability to speak has been reported in three previous patients with ZLS [de Pina Neto et al., 1988; Holzhausen et al., 2003; Shah et al., 2004]. Strabismus, seen in DGAP003, has also been noted previously [Van Buggenhout et al., 1995].

To refine the 3p14.3 breakpoint in the t(3;17), we performed FISH as previously described [Kim et al., 2005], using chromosome 3 specific BAC clones from genome maps provided by the University of California Santa Cruz (UCSC) Genomics Bioinformatics Group [Karolchik et al., 2003]. For the approximately 8.5 Mb region covering 3p14.2-p21.3, nine BAC clones were selected and hybridized to metaphase chromosomes from patient fibroblast cells (centromere to p arm telomere: RP11-180G14, RP11-229A12, RP11-169G24, RP11-39L1, RP11-58O15, RP11-452E8, RP11-189K9, RP11-122D19, RP11-3F4). Notably, BAC clone RP11-452E8 hybridized to the der(3), the der(17), and normal chromosome 3, indicating that this clone spans the breakpoint (Fig. 3). The size of the breakpoint region is estimated to be ~200 kb at 3p14.3, based upon the UCSC physical map. It is

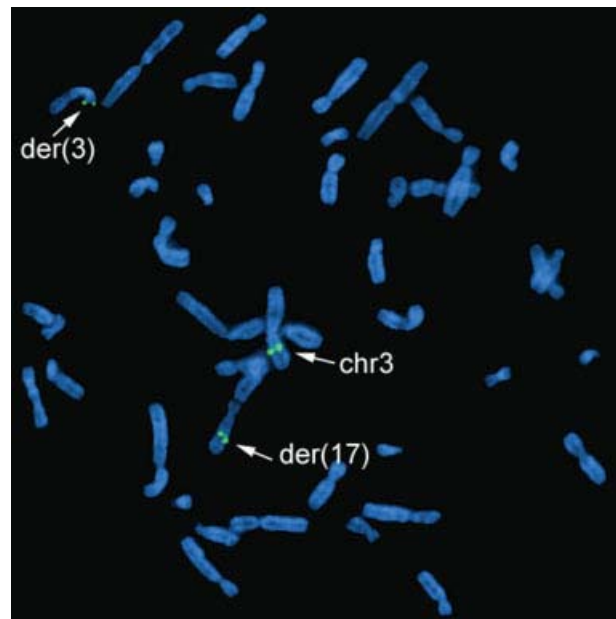


FIG. 3. FISH with BAC clone RP11-452E8 hybridized to metaphase spreads of DGAP003. Spectrum green-labeled BAC clone RP11-452E8 shows signals on the normal chromosome 3, der(3), and der(17), indicating that this BAC clone spans the 3p14.3 breakpoint.

important to note that one of the BACs used to delineate the 3p14.3 breakpoint of the t(3;8), RP11-189K9, flanks the breakpoint region of the 3;17 translocation on the distal side (Fig. 4), further suggesting that the gene for ZLS is located in this chromosomal region.

Based upon our FISH mapping data, *CACNA2D3* is directly disrupted by the translocation breakpoint and it is possible that *LRTM1* is interrupted, as well. However, it is well known that disease-associated chromosomal breaks can be positioned outside the relevant gene, thereby leading to altered expression of a neighboring gene [Kleinjan and van Heyningen, 2005]. The presence of such a position effect has been postulated, for instance, for a t(3;7)(q23;q32) in a patient presenting with the blepharophimosis/ptosis/epicanthus inversus syndrome. The causative gene, *FOXL2*, is located 180 kb distant from the breakpoint, which disrupts *C3orf15* at 3q23 [Crisponi et al., 2001]. Accordingly, in DGAP003, expression of *LRMT1* or any surrounding gene might be altered by a position effect of the 3p14.3 breakpoint.

*CACNA2D3* is directly disrupted and therefore the first candidate gene to be considered. It encodes a subunit of voltage-gated calcium channels, which, by permitting  $Ca^{2+}$  influx into cells, mediate many physiological processes, including neuronal excitability and muscle contraction [Catterall, 2000; Arikath and Campbell, 2003]. Interestingly, gingival hyperplasia is reported to be present in patients treated with calcium channel blockers, which affect intracellular calcium metabolism or transport [Missouris et al., 2000], suggesting the possibility of *CACNA2D3* dysfunction being involved in ZLS. The gene *LRTM1* (leucine-rich repeats and transmembrane domains 1), encodes a protein of unknown function; however, close proximity of this gene to the breakpoint makes it a strong positional candidate.

As hypertrichosis is a feature of ZLS, *WNT5A* emerges as another intriguing candidate gene, because it is expressed in developing and postnatal hair follicles, and is a known target of sonic hedgehog (SHH) during hair follicle morphogenesis [Reddy et al., 2001]. Furthermore, murine *Wnt5a* is

expressed in the outgrowing regions of the facial primordia including the frontonasal process and the distal regions of the digit perichondrium. Moreover, *Wnt5a*-deficient mice show absence of distal digits as well as abnormal outgrowth of the face [Yamaguchi et al., 1999]. Recently, *Wnt5a* and *Ror2*, an orphan receptor belonging to the family of receptor tyrosine kinases, were found to commonly activate the non-canonical Wnt pathway [Oishi et al., 2003]. Two allelic disorders are caused by mutations in *ROR2*. Brachydactyly type B, an autosomal dominant skeletal disorder characterized by hypoplasia/aplasia of the distal phalanges and nails [Oldridge et al., 2000; Schwabe et al., 2000] as well as a recessive form of Robinow syndrome manifesting with, for example, gingival hyperplasia [Teebi, 1990; Balci et al., 1998] and bifid terminal phalanges of the hands and feet [Giedion et al., 1976; Schwabe et al., 2004]. Notably, bilateral bipartite distal phalanx of the thumb was also reported in a ZLS patient [de Pina Neto et al., 1988]. Taken together, these data suggest an involvement of WNT5A-dependent signaling pathways in hair follicle morphogenesis, limb outgrowth, and development of gingival tissue, processes that are most likely impaired in patients with ZLS.

The gene *ERC2* (ELKS/RAB6-interacting/CAST family member 2) encodes a neuronal protein with four coiled-coil domains and a putative COOH-terminal consensus motif for binding to PDZ domains. It is associated with the cytomatrix at the active zone, beneath the presynaptic membrane, which is implicated in determining the site of synaptic vesicle fusion and neurotransmitter release [Ohtsuka et al., 2002]. *ERC2* is located in the center of the revised 3.2 Mb breakpoint region of the ZLS-associated t(3;8). Its relative proximity to the breakpoint region in DGAP003, makes it a positional candidate for ZLS.

The existence of two independent translocation breakpoints in 3p14.3 provides strong evidence that the causative gene for ZLS is located in this chromosomal region. Currently, we are performing mutation analysis of candidate genes in sporadic

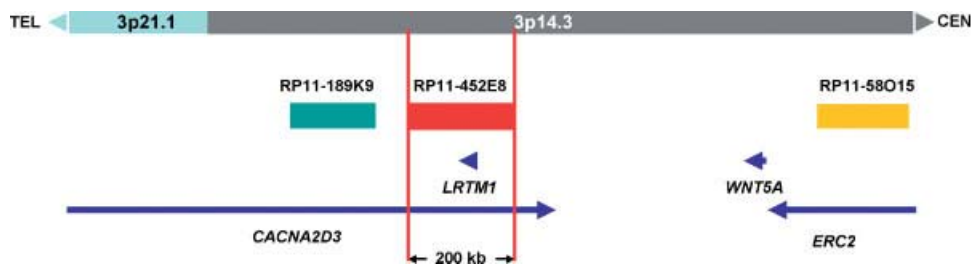


Fig. 4. Schematic representation of the breakpoint region at 3p14.3 in DGAP003. The upper line represents part of the region of 3p21.1 (light blue) to 3p14.3 (gray); telomere to centromere orientation is indicated. The figure is drawn to scale. The breakpoint spanning BAC clone RP11-452E8, delimiting the breakpoint region to 200 kb (indicated by two vertical red lines), is depicted in red, whereas the clones that mapped closest to the breakpoint on the proximal and distal side, respectively, are shown in yellow and green. Four possible candidate genes for ZLS are represented by thick blue arrows (indicating 5' → 3' orientation), with gene names indicated. The translocation breakpoint directly disrupts the *CACNA2D3* gene and possibly *LRTM1*.

patients with ZLS and normal karyotype to identify the underlying genetic defect.

### ACKNOWLEDGMENTS

We thank the individuals with ZLS and their families for their participation in this study. We are also indebted to Robert E. Eisenman and Diana J. Donovan for technical assistance, to Amy Bosco, Heather L. Ferguson, and Chantal Kelly for obtaining informed consent and clinical information. This work was supported by USPHS grants GM061354 (Developmental Genome Anatomy Project) and HD28138 and the Deutsche Forschungsgemeinschaft (KU 1240/3-1 and 3-2; K.K.).

### REFERENCES

- Alavandar G. 1965. Elephantiasis gingivae: Report of an affected family with associated hepatomegaly, soft tissue, and skeletal abnormalities. *J All India Dent Assoc* 37:349–353.
- Arikath J, Campbell KP. 2003. Auxiliary subunits: Essential components of the voltage-gated calcium channel complex. *Cur Opin Neurobiol* 13:298–307.
- Atabek ME, Pirgon O, Sert A, Toy H. 2005. Zimmermann–Laband syndrome in an infant with an atypical histologic finding. *Pediatr Dev Pathol* 8:654–657.
- Balci S, Beksac S, Haliloglu M, Ercis M, Eryilmaz M. 1998. Robinow syndrome, vaginal atresia, hematocolpos, and extra middle finger. *Am J Med Genet* 79:27–29.
- Bazopoulou-Kyrkanidou E, Papagianoulis L, Papanicolaou S, Mavrou A. 1990. Laband syndrome: A case report. *J Oral Pathol Med* 19:385–387.
- Catterall WA. 2000. Structure and regulation of voltage-gated Ca<sup>2+</sup> channels. *Annu Rev Cell Dev Biol* 16:521–555.
- Chodirker BN, Chudley AE, Toffler MA, Reed MH. 1986. Zimmerman–Laband syndrome and profound mental retardation. *Am J Med Genet* 25:543–547.
- Crisponi L, Deiana M, Loi A, Chiappe F, Uda M, Amati P, Bisceglia L, Zelante L, Nagaraja R, Porcu S, Ristaldi MS, Marzella R, Rocchi M, Nicolino M, Lienhardt-Roussie A, Nivelon A, Verloes A, Schlessinger D, Gasparini P, Bonneau D, Cao A, Pilia G. 2001. The putative forkhead transcription factor FOXL2 is mutated in blepharophimosis/ptosis/epicanthus inversus syndrome. *Nat Genet* 27:159–166.
- Davalos IP, Garcia-Cruz D, Garcia-Cruz MO, Ramirez-Duenas ML, Solis-Camara P, Correa-Cerro LS, Perez-Rulfo D, Sanchez-Corona J. 2005. Zimmermann–Laband syndrome: Further clinical delineation. *Genet Couns* 16:283–290.
- de Pina Neto JM, Soares LR, Souza AH, Petean EB, Velludo MA, de Freitas AC, Ribas JP. 1988. A new case of Zimmermann–Laband syndrome with mild mental retardation, asymmetry of limbs, and hypertrichosis. *Am J Med Genet* 31:691–695.
- Giedion A, Battaglia GF, Bellini F, Fanconi G. 1976. The radiological diagnosis of the fetal-face (=Robinow) syndrome (mesomelic dwarfism and small genitalia). Report of 3 cases. *Helv Paediatr Acta* 30:409–423.
- Holzhausen M, Goncalves D, Correa Fde O, Spolidorio LC, Rodrigues VC, Orrico SR. 2003. A case of Zimmermann–Laband syndrome with supernumerary teeth. *J Periodontol* 74:1225–1230.
- Il'ina EG, Lur'e IV, Vasiljuskene IP. 1988. Analysis of phenotypic variability of Zimmermann–Laband syndrome. *Pediatriia* 4: 86–88.
- Karolchik D, Baertsch R, Diekhans M, Furey TS, Hinrichs A, Lu YT, Roskin KM, Schwartz M, Sugnet CW, Thomas DJ, Weber RJ, Haussler D, Kent WJ. 2003. The UCSC genome browser database. *Nucleic Acids Res* 31:51–54.
- Kim HG, Herrick SR, Lemyre E, Kishikawa S, Salisz JA, Seminara S, MacDonald ME, Bruns GA, Morton CC, Quade BJ, Gusella JF. 2005. Hypogonadotropic hypogonadism and cleft lip and palate caused by a balanced translocation producing haploinsufficiency for FGFR1. *J Med Genet* 42:666–672.
- Kleinjan DA, van Heyningen V. 2005. Long-range control of gene expression: Emerging mechanisms and disruption in disease. *Am J Hum Genet* 76:8–32.
- Laband PF, Habib G, Humphreys GS. 1964. Hereditary gingival fibromatosis. Report of an affected family with associated splenomegaly and skeletal and soft-tissue abnormalities. *Oral Surg* 17:339–351.
- Missouris GG, Kalaitzidis RG, Cappuccio FP, MacGregor GA. 2000. Gingival hyperplasia caused by calcium channel blockers. *J Hum Hypertens* 14:155–156.
- Ohtsuka T, Takao-Rikitsu E, Inoue E, Inoue M, Takeuchi M, Matsubara K, Deguchi-Tawarada M, Satoh K, Morimoto K, Nakanishi H, Takai Y. 2002. Cast: A novel protein of the cytomatrix at the active zone of synapses that forms a ternary complex with RIM1 and munc13-1. *J Cell Biol* 158: 577–590.
- Oikawa K, Cavaglia AM, Lu D. 1979. Laband syndrome: Report of case. *J Oral Surg* 37:120–122.
- Oishi I, Suzuki H, Onishi N, Takada R, Kani S, Ohkawara B, Koshida I, Suzuki K, Yamada G, Schwabe GC, Mundlos S, Shibuya H, Takada S, Minami Y. 2003. The receptor tyrosine kinase Ror2 is involved in non-canonical Wnt5a/JNK signaling pathway. *Genes Cells* 8:645–654.
- Oldridge M, Fortuna AM, Maringa M, Propping P, Mansour S, Pollitt C, DeChiara TM, Kimble RB, Valenzuela DM, Yancopoulos GD, Wilkie AO. 2000. Dominant mutations in ROR2, encoding an orphan receptor tyrosine kinase, cause brachydactyly type B. *Nat Genet* 24:275–278.
- Pfeiffer RA, Seemanova E, Suss J, Müssig D, Tietze HU. 1992. The Zimmermann–Laband syndrome. *Klin Padiatr* 204:1–5.
- Reddy S, Andl T, Bagasra A, Lu MM, Epstein DJ, Morrisey EE, Millar SE. 2001. Characterization of Wnt gene expression in developing and postnatal hair follicles and identification of Wnt5a as a target of Sonic hedgehog in hair follicle morphogenesis. *Mech Dev* 107:69–82.
- Robertson SP, Lipp H, Bankier A. 1998. Zimmermann–Laband syndrome in an adult. Long-term follow-up of a patient with vascular and cardiac complications. *Am J Med Genet* 78:160–164.
- Schwabe GC, Tinschert S, Buschow C, Meinecke P, Wolff G, Gillissen-Kaesbach G, Oldridge M, Wilkie AO, Komec R, Mundlos S. 2000. Distinct mutations in the receptor tyrosine kinase gene ROR2 cause brachydactyly type B. *Am J Hum Genet* 67:822–831.
- Schwabe GC, Trepczyk B, Suring K, Brieske N, Tucker AS, Sharpe PT, Minami Y, Mundlos S. 2004. Ror2 knockout mouse as a model for the developmental pathology of autosomal recessive Robinow syndrome. *Dev Dyn* 229:400–410.
- Shah N, Gupta YK, Ghose S. 2004. Zimmermann–Laband syndrome with bilateral developmental cataract—A new association? *Int J Paediatr Dent* 14:78–85.
- Stefanova M, Atanassov D, Krastev T, Fuchs S, Kutsche K. 2003. Zimmermann–Laband syndrome associated with a balanced reciprocal translocation t(3;8)(p21.2;q24.3) in mother and daughter: Molecular cytogenetic characterization of the breakpoint regions. *Am J Med Genet Part A* 117A:289–294.
- Teebi AS. 1990. Autosomal recessive Robinow syndrome. *Am J Med Genet* 35:64–68.
- Van Buggenhout GJ, Brunner HG, Trommelen JC, Hamel BC. 1995. Zimmermann–Laband syndrome in a patient with severe mental retardation. *Genet Couns* 6:321–327.
- Yamaguchi TP, Bradley A, McMahon AP, Jones S. 1999. A Wnt5a pathway underlies outgrowth of multiple structures in the vertebrate embryo. *Development* 126:1211–1223.
- Zimmermann KW. 1928. Ueber Anomalien des Ektoderms. *Vjschr Zahnheilk* 44:419–434.

# Extensive Molecular Genetic Analysis of the 3p14.3 Region in Patients With Zimmermann–Laband Syndrome

Benjamin Abo-Dalo,<sup>1</sup> Hyung-Goo Kim,<sup>2</sup> Melanie Roes,<sup>1</sup> Margarita Stefanova,<sup>1,3</sup>  
Anne Higgins,<sup>4</sup> Yiping Shen,<sup>2</sup> Stefan Mundlos,<sup>5</sup> Bradley J. Quade,<sup>4</sup>  
James F. Gusella,<sup>2</sup> and Kerstin Kutsche<sup>1\*</sup>

<sup>1</sup>Institut für Humangenetik, Universitätsklinikum Hamburg-Eppendorf, Hamburg, Germany

<sup>2</sup>Molecular Neurogenetics Unit, Center for Human Genetic Research, Massachusetts General Hospital/Department of Genetics, Harvard Medical School, Massachusetts

<sup>3</sup>Department of Medical Genetics, Medical University, Plovdiv, Bulgaria

<sup>4</sup>Department of Pathology, Brigham and Women's Hospital/Harvard Medical School, Boston, Massachusetts

<sup>5</sup>Max-Planck Institute for Molecular Genetics, Ihnestr. 1, Berlin, Germany

Received 21 March 2007; Accepted 17 June 2007

Zimmermann–Laband syndrome (ZLS) is a rare autosomal dominant inherited disorder characterized by a coarse facial appearance, gingival fibromatosis, and absence or hypoplasia of the terminal phalanges and nails of hands and feet. Additional, more variable features include hyperextensibility of joints, hepatosplenomegaly, mild hirsutism, and mental retardation. Mapping of the translocation breakpoints of t(3;8) and t(3;17) found in patients with the typical clinical features of ZLS defined a common breakpoint region of ~280 kb located in 3p14.3, which includes the genes *CACNA2D3* and *WNT5A*. Breakpoint cloning revealed that both translocations most likely occurred by non-homologous (illegitimate) recombination. Mutation analysis of nine genes located in 3p21.1-p14.3, including *CACNA2D3*, which is directly disrupted by one breakpoint of the t(3;17), identified no pathogenic mutation in eight sporadic patients with ZLS. Southern hybridization analysis and multiplex ligation-dependent probe amplification (MLPA) did not

detect submicroscopic deletion or duplication in either *CACNA2D3* or *WNT5A* in ZLS-affected individuals. Mutation analysis of nine conserved nongenic sequence elements (CNEs) in 3p21.1-p14.3, which were identified by interspecies comparison and may represent putative regulatory elements for spatiotemporally correct expression of nearby genes, did not show any sequence alteration associated with ZLS. Taken together, the lack of a specific coding-sequence lesion in the common region, defined by two translocation breakpoints, in sporadic patients with ZLS and an apparently normal karyotype suggests that either some other type of genetic defect in this vicinity or an alteration elsewhere in the genome could be responsible for ZLS. © 2007 Wiley-Liss, Inc.

**Key words:** Zimmermann–Laband syndrome; *WNT5A*; *CACNA2D3*; chromosome translocation; gingival hyperplasia

**How to cite this article:** Abo-Dalo B, Kim H-G, Roes M, Stefanova M, Higgins A, Shen Y, Mundlos S, Quade BJ, Gusella JF, Kutsche K. 2007. Extensive molecular genetic analysis of the 3p14.3 region in patients with Zimmermann–Laband syndrome. *Am J Med Genet Part A* 143A:2668–2674.

## INTRODUCTION

Zimmermann–Laband syndrome (ZLS) (OMIM 135500) is a rare disorder which is mainly character-

ized by a coarse facial appearance including bulbous soft nose, thickened lips, thick and floppy ears, gingival hypertrophy or fibromatosis, aplasia

This article contains supplementary material, which may be viewed at the American Journal of Medical Genetics website at <http://www.interscience.wiley.com/jpages/1552-4825/suppmat/index.html>.

Benjamin Abo-Dalo and Hyung-Goo Kim contributed equally to this work.

Hyung-Goo Kim's present address is CB2803, IMMAG, Medical College of Georgia, 1120 15th Street, Augusta, GA 30912.

The results summarized here are part of the Ph.D. thesis of Benjamin Abo-Dalo and of the M.D. thesis of Melanie Roes at the University of Hamburg.

Grant sponsor: Deutsche Forschungsgemeinschaft; Grant numbers: GRK336, KU 1240/3-1, 3-2; Grant sponsor: DAAD; Grant number: DAAD 07/2005; Grant sponsor: USPHS; Grant numbers: GM061354, HD28138.

\*Correspondence to: Kerstin Kutsche, Ph.D., Institut für Humangenetik, Universitätsklinikum Hamburg-Eppendorf, Campus Forschung, Gebäude 146, Martinistraße 52, D-20246 Hamburg, Germany.

E-mail: [kkutsche@uke.uni-hamburg.de](mailto:kkutsche@uke.uni-hamburg.de)

DOI 10.1002/ajmg.a.32034

or dysplasia of hand- and toenails, and various skeletal anomalies including hypoplastic changes of the terminal phalanges and hyperextensibility of joints [Chodirker et al., 1986; Pfeiffer et al., 1992; Van Buggenhout et al., 1995]. ZLS is most likely inherited as an autosomal dominant disorder with de novo mutations in sporadic cases [Laband et al., 1964; Alavandar, 1965]. The occurrence of a 3;8 translocation in mother and daughter, both of which presented with the typical features of ZLS, further supports this mode of inheritance [Stefanova et al., 2003]. Breakpoint mapping of a de novo 3;17 translocation in a male with features characteristic of ZLS indicated that the 3p14.3 breakpoint of both cases may be shared, suggesting that a gene causative for ZLS is located in this region [Kim et al., 2007]. By fluorescence in situ hybridization (FISH) analysis, one BAC clone was found to span the 3p14.3 breakpoint of the t(3;17), thereby directly disrupting the *CACNA2D3* gene [Kim et al., 2007]. *CACNA2D3* encodes the auxiliary  $\alpha_{2\delta-3}$  subunit part of the voltage-gated  $Ca^{2+}$  channel which is implicated in a wide range of physiological processes [Felix, 2006]. Remarkably, calcium channel blockers can induce gingival overgrowth [Kataoka et al., 2005], suggesting that *CACNA2D3* dysfunction might be involved in ZLS. Another candidate gene, *WNT5A*, is located ~550 kb centromeric to the 3p breakpoint of the t(3;17) [Kim et al., 2007]. It encodes a secretory glycoprotein that plays an important role during the formation and growth of multiple structures and tissues in mice and is a target of Sonic hedgehog (Shh) in hair follicle morphogenesis [Yamaguchi et al., 1999; Reddy et al., 2001]. Thus, *WNT5A* also is a positional and functional candidate for ZLS.

Breakpoints of chromosomal translocations may be positioned outside of a pathogenic gene, and yet still give rise to a particular disease phenotype. Such rearrangements cause either direct disruption of *cis* regulatory elements required for normal gene transcription or physical dissociation of the transcribed gene from these regulatory elements. In either case, subsequent aberrant gene transcription can lead to human disease [Kleinjan and van Heyningen, 1998; Kleinjan and van Heyningen, 2005]. *Cis*-acting genomic elements can stretch up to 1 Mb in either direction from the transcription unit and thus, translocation breakpoints can be located far away from the disease gene. For example, an evolutionary conserved nongenic element (CNE) located 1 Mb upstream of the *Sbb* gene was found to function as a limb-specific enhancer element required for its proper expression [Lettice et al., 2002, 2003]. Remarkably, single base pair substitutions in this element have been identified in members of four families affected by preaxial polydactyly as well as two mouse mutants [Lettice et al., 2003; Sagai et al., 2004], suggesting that mutations in *cis* regulatory elements can result in the same phenotypic outcome

as observed in patients with chromosomal translocations.

Here, we report on breakpoint cloning of two chromosome translocation cases with ZLS as well as detailed molecular analysis of genes and CNEs, representing putative *cis* regulatory elements, all located in and around the 3p14.3 breakpoint region in individuals with sporadic ZLS and an apparently normal karyotype.

## MATERIALS AND METHODS

### Subjects

The translocation patients with t(3;8) and t(3;17) were described elsewhere [Stefanova et al., 2003; Kim et al., 2007]. We collected DNA, blood samples, or EBV-transformed lymphoblastoid cell lines from eight patients clinically diagnosed with ZLS. Five of the eight patients have been reported previously [de Pina Neto et al., 1988; Koch et al., 1992; Pfeiffer et al., 1992; Robertson et al., 1998]. The three novel patients show the typical ZLS-specific features, such as hypoplastic or aplastic terminal phalanges, aplastic nails, gingival fibromatosis, and a coarse face with bulbous nose, full lips, and macroglossia. Clinical data of seven patients will be published elsewhere [Abo-Dalo et al., 2007]. Conventional cytogenetic analysis revealed an apparently normal karyotype for all individuals.

Our ethics committees approved this study, and written informed consent was obtained from all participants or their legal guardians.

### Fluorescence In Situ Hybridization (FISH)

Metaphase spreads from peripheral blood lymphocytes, lymphoblastoid cells, or fibroblasts were made by standard procedure. Chromosome 3-specific fosmid clones from library G248P8 (3531E12, 4994D9, 423A8, 5972G4, 2432H1, 6512A3, 2004A7, 3425E7, and 405C7) were obtained from BACPAC Resources (Children's Hospital Oakland, Oakland, CA), while BAC clone 889D3 from the RPCI11-library was provided by the Resource Center of the German Human Genome Project at the Max-Planck-Institute for Molecular Genetics, Berlin, Germany. Isolation and labeling of fosmid and BAC DNA as well as FISH was performed as described previously [Sutajova et al., 2004].

### PCR on Genomic DNA

Genomic DNA was isolated from peripheral blood samples, fibroblast, or lymphoblastoid cells of the translocation patients by standard procedures. For breakpoint cloning of the t(3;8) and t(3;17), we amplified specific junction fragments that were directly sequenced. Primer sequences are available on request.

### Mutation Screening of Genes in 3p14.3 (*CHDH*, *IL17RB*, *ACTR8*, *SELK*, *CACNA2D3*, *LRTM1*, *ERC2*, *CCDC66*, and *C3orf63*) and 8q24.3 (*NIBP*, *EIF2C2*, *KCNK9*, *CHRAC1*, *C8orf17*, and *MIRN151*)

We amplified the coding region including the flanking intronic sequences of the following genes from genomic DNA. Exon number in parentheses provides the number of screened coding exons for each gene: *CHDH* (7 exons; GenBank accession no. NM\_018397), *IL17RB* (11 exons; GenBank accession no. NM\_018725 and NM\_172234), *ACTR8* (13 exons; GenBank accession no. NM\_022899), *SELK* (5 exons; GenBank accession no. NM\_021237), *CACNA2D3* (38 exons; GenBank accession no. NM\_018398), *LRTM1* (3 exons; GenBank accession no. NM\_020678), *ERC2* (16 exons; GenBank accession no. NM\_015576), *CCDC66* (15 exons; GenBank accession no. NM\_001012506), *C3orf63* (15 exons; GenBank accession no. NM\_015224), *NIBP* (23 exons; GenBank accession no. NM\_031466.3), *EIF2C2* (20 exons; GenBank accession no. NM\_012154.2), *KCNK9* (2 exons; GenBank accession no. NM\_016601.2), *CHRAC1* (3 exons; GenBank accession no. NM\_017444.3), *C8orf17* (1 exon; GenBank accession no. NM\_020237.1), and *MIRN151* (1 exon; GenBank accession no. NT\_008046.15: 54960842–54960931 bp). Primer sequences and PCR conditions are available on request. PCR products were directly sequenced with the Big Dye Terminator ready reaction kit (PE Applied Biosystems, Darmstadt, Germany) on an ABI Prism 377 (PE Applied Biosystems).

### Southern Blot Analysis

Southern blot analysis using various restriction enzymes was carried out using standard protocols [Kim et al., 2005]. Four hybridization probes were generated using four primer sets covering a 41-kb region encompassing the complete genomic region of *WNT5A* (22 kb). Primer sequences are available upon request.

### Multiplex Ligation-Dependent Probe Amplification (MLPA)

The MLPA probes were designed according to the described guideline [Schouten et al., 2002]. For *CACNA2D3*, pairs of synthetic MLPA probes were designed from twelve selected coding exons, whereas six pairs of synthetic MLPA probes were designed for *WNT5A*, including four for coding exons and one each for the 5'- and 3'-UTR. In addition, two pairs of control probes were designed. Amplification product sizes ranged from 92 to 117 bp; all have similar melting temperatures. MLPA reagents were obtained from MRC-Holland; the EK1 kit and reactions were used according to the manufacturer's instructions.

### Comparative Sequence Analysis for the Identification of Conserved Nongenic Elements (CNEs) and Mutation Analysis

CNEs 1–9 located distal to the breakpoint in 3p14.3 of the t(3;8) were obtained by sequence alignments between the species human, mouse, chicken, *Xenopus laevis*, and *Tetraodon nigroviridis* using the MultiPIPMaker program [Schwartz et al., 2000] (<http://bio.cse.psu.edu/>). Sequences were obtained from ENSEMBL (<http://www.ensembl.org>).

Using *Homo sapiens* chromosome 3 genomic contig NT\_022517.17 as the reference sequence, we amplified CNE1 (54230851–54231688 bp), CNE2 (54644200–54644846 bp), CNE3 (54707163–54708044 bp), CNE4 (54747357–54747820 bp), CNE5 (54832588–54833367 bp), CNE6 (54957772–54958525 bp), CNE7 (55001613–55002698 bp), CNE8 (55217983–55218938 bp), and CNE9 (55296646–55297676 bp) and directly sequenced them. Primer sequences and PCR conditions are available on request.

### Quantitative Real Time RT-PCR

Quantitative real time RT-PCR (Q-RT-PCR) was performed using total RNA isolated from synchronized lymphoblastoid cells lines (LCLs). Therefore,  $3 \times 10^5$  cells were cultured in RPMI 1640 medium supplemented with 20% FBS (Gibco, Karlsruhe, Germany). For starvation,  $6 \times 10^6$  cells were incubated in medium supplemented with 1% FBS for 30 hr, following 18 hr in medium without FBS. Subsequently, RNA was extracted using Qiashredder (QIAGEN, Hilden, Germany) and the RNeasy Kit (QIAGEN) according to the manufacturer's instructions. One microgram of RNA of each sample was reverse transcribed into cDNA (Superscript II<sup>®</sup>, Invitrogen, Karlsruhe, Germany) using a cocktail of gene-specific primers. Q-RT-PCR was performed in a 20  $\mu$ l reaction containing 3  $\mu$ l of 1:5 diluted cDNA, 1.6  $\mu$ l primer mix (8  $\mu$ M of each primer), and 10  $\mu$ l SYBR<sup>®</sup> Green JumpStart<sup>™</sup> Taq ReadyMix<sup>™</sup> (Sigma, Taufkirchen, Germany). Assays (n = 3) were performed in duplicates on a Rotorgene-3000 (Corbett Research, Sydney, Australia). We calculated expression levels using the efficiency  $\Delta\Delta C(T)$ -method [Pfaffl, 2001] and *HPRT* as reference transcript. Primer sequences are available on request.

### RESULTS

We delineated the 3p14.3 breakpoint region of the t(3;8) by FISH and identified BAC RP11-889D3 and the two fosmids 2004A7 and 3425E7 spanning the breakpoint (data not shown and Fig. 1A). The chromosome 3 breakpoint of the t(3;17), which was found to disrupt the *CACNA2D3* gene [Kim et al., 2007], was refined with fosmid 423A8 (data not

shown and Fig. 1A). Both 3p14.3 breakpoints mapped within a common region of ~280 kb, and the t(3;8) breakpoint does not seem to interrupt a gene (Fig. 1B). Instead, the latter one potentially cause a position effect on an adjacent gene, which include *CACNA2D3*, *LRTM1*, *WNT5A*, and *ERC2*, in order of proximity to the chromosome 3 breakpoint (Fig. 1B).

To map further the breakpoints of the translocation partners at 8q24.3 and 17q24.3, FISH with overlapping fosmids was performed (data not shown). Based on that data, a series of PCR reactions for the four derivative chromosomes were performed to amplify junction-specific amplicons in individuals with translocations, but not in normal controls (Fig. 2A, B).

Sequence analysis of the breakpoint-spanning junction fragments of the t(3;8) revealed that both chromosomal breaks occurred in single copy DNA, nonetheless, the breakpoint in 3p14.3 is distally and proximally flanked by MIR repeats (data not shown). At the junction of the der(8), an overlap of 3 bp (CTC) was found, while a deletion of 8–11 bp of chromosome 8 and 9–12 bp of chromosome 3 material was detected on the der(3) (Fig. 2C). We amplified and sequenced breakpoint-spanning amplicons for both derivatives of the t(3;17) and identified the 3p14.3 breakpoint in intron 27 of *CACNA2D3*. The *LRTM1* gene, located in intron 27 of *CACNA2D3* in reverse orientation, was not found to be interrupted. The 3p14.3 breakpoint occurred

in single copy DNA, whereas that in 17q24.3 in a LINE repeat (data not shown). We detected a 12-bp deletion encompassing 11 bp of chromosome 3 and 1 bp of chromosome 17 material on the der(17) (Fig. 2D). Taken together, both translocations are unbalanced on the molecular level and most likely occurred by non-homologous non-allelic recombination [Abeysinghe et al., 2003].

We performed mutation screening of the coding exons of nine genes located in the breakpoint region of 3p21.1-p14.3 (*CHDH*, *IL17RB*, *ACTR8*, *SELK*, *CACNA2D3*, *LRTM1*, *ERC2*, *CCDC66*, and *C3orf63*; Fig. 1B) in eight patients with ZLS. *WNT5A* has been analyzed previously and did not show any sequence alteration associated with ZLS [Abo-Dalo et al., 2007]. Numerous sequence variants were identified in both intronic and coding regions for eight of the nine genes studied. However, they were found either in healthy controls or unaffected members of the patients' families indicating that they most likely represent polymorphisms (see the online Table I at <http://www.interscience.wiley.com/jpages/1552-4825/suppmat/index.html>).

Next, we tested for copy number anomalies and submicroscopic rearrangements for the two most promising genes in 3p21.1-p14.3, *CACNA2D3* and *WNT5A*. First, Southern hybridization analysis did not reveal any aberrant band in three patients with ZLS compared with control samples (data not shown). Second, by using MLPA we analyzed the gene dosage of *CACNA2D3* (exons 1, 4, 5, 8, 11, 13,

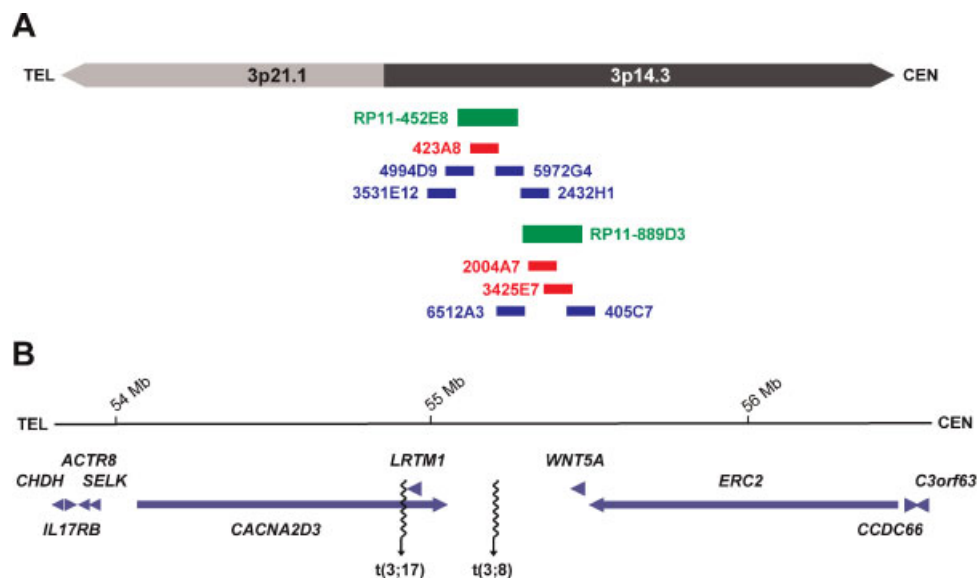


Fig. 1. Both 3p breakpoints of the t(3;8) and t(3;17) map within a region of ~280 kb in p14.3. **A:** Schematic representation of the breakpoint region at 3p14.3. The upper bar represents part of the 3p21.1 (light gray) and 3p14.3 (dark gray) regions. Telomere to centromere orientation is indicated. The breakpoint spanning BAC clone RP11-452E8 and RP11-889D3 of the t(3;17) and t(3;8), respectively, is depicted by a green bar. Fosmid 423A8, spanning the breakpoint of the t(3;17), is shown as red bar below BAC RP11-452E8. Clones mapping either distal (4994D9 and 3531E12) or proximal (5972G4 and 2432H1) to the breakpoint are depicted in blue. For the t(3;8) breakpoint, two fosmids, 2004A7 and 3425E7, that span the breakpoint, are indicated as red bars below BAC RP11-889D3. Clones mapping closest to the breakpoint on the distal (6512A3) and proximal (405C7) side, respectively, are shown as blue bars. **B:** Schematic representation of genes located in the 3p14.3 breakpoint region. The upper line represents a region in 3p21.1-p14.3 in telomere (TEL) to centromere (CEN) orientation; sizes in Mb are shown. Genes are depicted as blue arrows or arrow heads (indicating 5' → 3' orientation) and gene names are given. Breakpoints of the t(3;8) and t(3;17) are indicated by wavy lines. [Color figure can be viewed in the online issue, which is available at [www.interscience.wiley.com](http://www.interscience.wiley.com).]

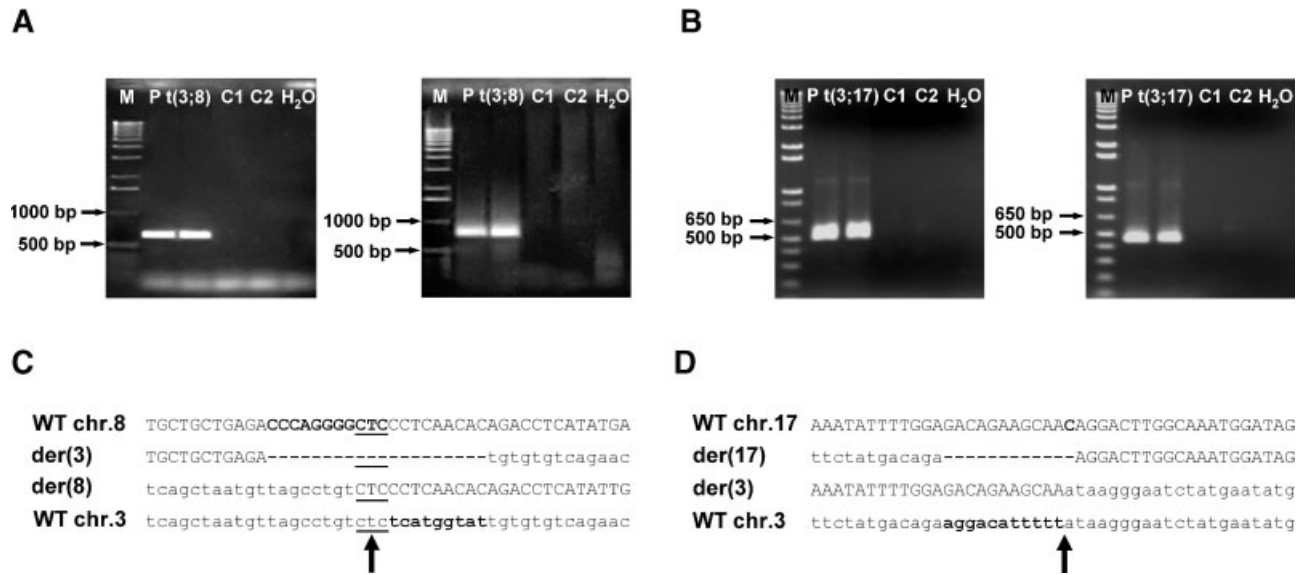


FIG. 2. Characterization of both the t(3;8) and t(3;17) translocation breakpoints at the genomic DNA level. **A:** Amplification of junction fragments for both der(3) and der(8) chromosomes. A fragment of ~700 bp was obtained from the der(8) of the mother carrying t(3;8) [P t(3;8); doublet], but not in controls (C1, C2) (left panel). Junction fragment amplification of the der(3) chromosome yielded a fragment of ~800 bp from the patient [P t(3;8); doublet] that was not observed in controls (C1, C2) (right panel). One kilobase ladder (M) was used as DNA size marker. **B:** Junction fragments of both derivative chromosomes of the t(3;17) amplified by PCR. A ~550-bp fragment was obtained from the derivative chromosome 17 of the t(3;17) patient [P t(3;17); doublet], but not in controls (C1, C2) (left panel). Junction fragment amplification of the der(3) yielded a fragment of ~500 bp from the translocation patient [P t(3;17); doublet] that was not observed in healthy individuals (C1, C2). Sizes of two bands of the DNA size marker (M) are indicated. **C, D:** Sequence alignment of the derivative and wild-type sequences of the t(3;8) (C) and t(3;17) (D), respectively, at the translocation breakpoints. Chromosome 8- and chromosome 17-derived sequences are shown in uppercase letters, those from chromosome 3 in lowercase letters. The breakpoint region is indicated by an arrow. Nucleotides deleted in the der(3) and der(17), respectively, are shown in bold in the respective wild-type sequence. C: Overlapping sequence at the breakpoint is underlined.

19, 26, 28, 30, 34, and 36) in six ZLS-affected patients and of *WNT5A* (four coding exons and 5'- and 3'-UTR) in eight patients with ZLS. No differences in the dosage of the analyzed exons in the patients compared with controls were found (data not shown). These data suggest that deletions, duplications, or inversions in *CACNA2D3* or *WNT5A* may not account for the disease phenotype in the chromosomally normal ZLS-affected patients analyzed.

To test altered transcriptional regulation for a gene near the chromosome 3 breakpoint, we determined gene expression level of *WNT5A* and the two neighboring genes *CACNA2D3* and *LRTM1* by Q-RT-PCR. Expression level of *CACNA2D3* and *LRTM1* was too low to be determined (data not shown). Notably, mRNA levels for *WNT5A* were found to show a high variation in unrelated controls, precluding the comparison of its expression levels in patients with ZLS with those from controls (data not shown).

To identify CNEs, which may serve as putative long-range regulatory elements for various genes in 3p21.1-p14.3, we performed multiple sequence comparisons between evolutionary divergent species and found nine cross-species conserved elements (CNE1–CNE9) that spread across the analyzed region (see the online Fig. 1A,B at <http://www.interscience.wiley.com/jpages/1552-4825/suppmat/index.html>). We performed mutation analysis of CNEs 1–9 in eight patients with ZLS and identified seven single base pair substitutions which do not

seem to be associated with ZLS (see the online Fig. 1C at <http://www.interscience.wiley.com/jpages/1552-4825/suppmat/index.html>).

## DISCUSSION

In this study, we most likely excluded pathogenic mutations in 3p21.1-p14.3 as a cause of ZLS in individuals without chromosomal rearrangement involving this region. It is possible, however, that some cryptic genetic defect remains to be discovered in this region. For example, mutations in non-coding RNAs (e.g., microRNAs) could be present. The respective genes produce functional RNAs instead of proteins and have been involved in numerous biological processes as well as linked to human disease [Mattick and Makunin, 2006; Mehler and Mattick, 2006]. In addition, other cryptic alterations such as microdeletions in not yet analyzed regions in 3p21.1-p14.3, changes in the 5'- or 3'-UTR of a specific gene, or promoter defects might have escaped detection by the thorough methods employed. Nonetheless, heterozygous alterations in *WNT5A*, the most promising candidate, are most likely not causative for the autosomal dominant inherited ZLS. In line with this finding, mutations in two members of the WNT family have been reported in monogenic disorders with autosomal recessive inheritance in humans [Niemann et al., 2004; Woods et al., 2006] and mice [Parr and McMahon,

1995; Yamaguchi et al., 1999; Barrow et al., 2003]. However, we cannot exclude the possibility that the 3p14.3 breakpoints of the two translocations separate *WNT5A* from several regulatory elements causing down- and/or dysregulation of its expression that leads to ZLS in these cases.

We identified no pathogenic alteration in *CACNA2D3* in ZLS-affected patients. Concordantly, *Cacna2d3* knock-out mice do not share phenotypic features with patients with ZLS as they show a decreased startle reflex and increased aggression and hyperactivity in a small number of homozygotes ([http://www.informatics.jax.org/searches/accession\\_report.cgi?id=MGI:3604520](http://www.informatics.jax.org/searches/accession_report.cgi?id=MGI:3604520)).

Alternatively, the gene for ZLS could be carried on one of the other translocation partners. Interestingly, a patient with clinical features of ZLS has recently been described to carry an insertion of the chromosome 8 segment q11.2-q24.3 into p11.2 of chromosome 12 [Hoogendijk et al., 2006]. Thus, one breakpoint of the inserted fragment (i.e., 8q24.3) corresponds well to the 8q24.3 breakpoint of the t(3;8). In fact, delineation of this breakpoint identified the *NIBP* gene to be directly disrupted. However, mutation analysis of *NIBP* and five neighboring genes (*KCNK9*, *EIF2C2*, *CHRAC1*, *C8orf17*, and *MIRN151*) in eight ZLS-affected individuals revealed that none of the 25 detected sequence variations is causative for the disease.

Based on the lack of a specific genetic lesion in 3p14.3 and 8q24.3 in sporadic patients with ZLS, we suggest that either a cryptic genetic defect in the vicinity of the breakpoint(s) in 3p14.3 and 8q24.3, respectively, or an alteration elsewhere in the genome might be associated with ZLS. Nonetheless, the situation in ZLS might also resemble that in thrombocytopenia-absent radius (TAR) syndrome, for which a complex inheritance pattern with at least two unlinked alleles seems to be required to manifest the phenotype [Klopocki et al., 2007]. Similarly, a modifier located on 3p14.3 could be necessary to elicit the full-blown ZLS phenotype, while the genetic defect, which is the prerequisite for development of the disease, still has to be discovered.

#### ACKNOWLEDGMENTS

We are grateful to the patients and families who participated in this study. We are indebted to Inka Jantke, Robert E. Eisenman, and Diana J. Donovan for skillful technical assistance, Heather L. Ferguson and Chantal Kelly for obtaining informed consent and clinical information, Steven R. Herrick for help with FISH mapping, Alexander Linev for help with mutation analysis, and Michael Niedermaier for MultiPIPMaker analysis. This work was supported by grants from the Deutsche Forschungsgemeinschaft (GRK336, KU 1240/3-1 and 3-2 to K.K.), the DAAD (DAAD 07/2005 to M.S.), and USPHS grants GM

061354 (Developmental Genome Anatomy Project) and HD28138 (to J.F.G.).

#### REFERENCES

- Abeyasinghe SS, Chuzhanova N, Krawczak M, Ball EV, Cooper DN. 2003. Translocation and gross deletion breakpoints in human inherited disease and cancer I: Nucleotide composition and recombination-associated motifs. *Hum Mutat* 22:229–244.
- Alavandar G. 1965. Elephantiasis gingivae. Report of an affected family with associated hepatomegaly, soft tissue & skeletal abnormalities. *J All India Dent Assoc* 37:349–353.
- Barrow JR, Thomas KR, Boussadia-Zahui O, Moore R, Kemler R, Capecchi MR, McMahon AP. 2003. Ectodermal Wnt3/beta-catenin signaling is required for the establishment and maintenance of the apical ectodermal ridge. *Genes Dev* 17:394–409.
- Chodirker BN, Chudley AE, Toffler MA, Reed MH. 1986. Zimmerman–Laband syndrome and profound mental retardation. *Am J Med Genet* 25:543–547.
- de Pina Neto JM, Soares LR, Souza AH, Petean EB, Velludo MA, de Freitas AC, Ribas JP. 1988. A new case of Zimmerman–Laband syndrome with mild mental retardation, asymmetry of limbs, and hypertrichosis. *Am J Med Genet* 31:691–695.
- Felix R. 2006. Calcium channelopathies. *Neuromolecular Med* 8:307–318.
- Hoogendijk CF, Marx J, Honey EM, Pretorius E, Christianson AL. 2006. Ultrastructural investigation of Zimmerman–Laband syndrome. *Ultrastruct Pathol* 30:423–426.
- Kataoka M, Kido J, Shinohara Y, Nagata T. 2005. Drug-induced gingival overgrowth—a review. *Biol Pharm Bull* 28:1817–1821.
- Kim HG, Herrick SR, Lemyre E, Kishikawa S, Salisz JA, Seminara S, MacDonald ME, Bruns GA, Morton CC, Quade BJ, Gusella JF. 2005. Hypogonadotropic hypogonadism and cleft lip and palate caused by a balanced translocation producing haploinsufficiency for FG FR1. *J Med Genet* 42:666–672.
- Kim HG, Higgins AW, Herrick SR, Kishikawa S, Nicholson L, Kutsche K, Ligon AH, Harris DJ, Macdonald ME, Bruns GA, Morton CC, Quade BJ, Gusella JF. 2007. Candidate loci for Zimmerman–Laband syndrome at 3p14.3. *Am J Med Genet Part A* 143A:107–111.
- Kleinjan DJ, van Heyningen V. 1998. Position effect in human genetic disease. *Hum Mol Genet* 7:1611–1618.
- Kleinjan DA, van Heyningen V. 2005. Long-range control of gene expression: Emerging mechanisms and disruption in disease. *Am J Hum Genet* 76:8–32.
- Klopocki E, Schulze H, Strauss G, Ott CE, Hall J, Trotier F, Fleischhauer S, Greenhalgh L, Newbury-Ecob RA, Neumann LM, Habenicht R, König R, Seemanova E, Megarbane A, Ropers HH, Ullmann R, Horn D, Mundlos S. 2007. Complex inheritance pattern resembling autosomal recessive inheritance involving a microdeletion in thrombocytopenia-absent radius syndrome. *Am J Hum Genet* 80:232–240.
- Koch P, Wettstein A, Knauber J, Zaun H. 1992. A new case of Zimmerman–Laband syndrome with atypical retinitis pigmentosa. *Acta Derm Venereol* 72:376–379.
- Laband PF, Habib G, Humphreys GS. 1964. Hereditary Gingival Fibromatosis. Report of an affected family with associated splenomegaly and skeletal and soft-tissue abnormalities. *Oral Surg Oral Med Oral Pathol* 17:339–351.
- Lettice LA, Horikoshi T, Heaney SJ, van Baren MJ, van der Linde HC, Breedveld GJ, Joosse M, Akarsu N, Oostra BA, Endo N, Shibata M, Suzuki M, Takahashi E, Shinka T, Nakahori Y, Ayusawa D, Nakabayashi K, Scherer SW, Heutink P, Hill RE, Noji S. 2002. Disruption of a long-range cis-acting regulator for Shh causes preaxial polydactyly. *Proc Natl Acad Sci USA* 99:7548–7553.
- Lettice LA, Heaney SJ, Purdie LA, Li L, de Beer P, Oostra BA, Goode D, Elgar G, Hill RE, de Graaff E. 2003. A long-range Shh enhancer regulates expression in the developing limb and fin

- and is associated with preaxial polydactyly. *Hum Mol Genet* 12:1725–1735.
- Mattick JS, Makunin IV. 2006. Non-coding RNA. *Hum Mol Genet* 15:R17–R29.
- Mehler MF, Mattick JS. 2006. Non-coding RNAs in the nervous system. *J Physiol* 575:333–341.
- Niedermaier M, Schwabe GC, Fees S, Helmrich A, Brieske N, Seemann P, Hecht J, Seitz V, Stricker S, Leschik G, Schrock E, Selby PB, Mundlos S. 2005. An inversion involving the mouse *Shh* locus results in brachydactyly through dysregulation of *Shh* expression. *J Clin Invest* 115:900–909.
- Niemann S, Zhao C, Pasco F, Stahl U, Aulepp U, Niswander L, Weber JL, Muller U. 2004. Homozygous *WNT3* mutation causes tetra-amelia in a large consanguineous family. *Am J Hum Genet* 74:558–563.
- Parr BA, McMahon AP. 1995. Dorsalizing signal *Wnt-7a* required for normal polarity of D-V and A-P axes of mouse limb. *Nature* 374:350–353.
- Pfaffl MW. 2001. A new mathematical model for relative quantification in real-time RT-PCR. *Nucleic Acids Res* 29:45.
- Pfeiffer RA, Seemanova E, Suss J, Mussig D, Tietze HU. 1992. The Zimmermann–Laband syndrome. *Klin Padiatr* 204:1–15.
- Reddy S, Andl T, Bagasra A, Lu MM, Epstein DJ, Morrisey EE, Millar SE. 2001. Characterization of *Wnt* gene expression in developing and postnatal hair follicles and identification of *Wnt5a* as a target of Sonic hedgehog in hair follicle morphogenesis. *Mech Dev* 107:69–82.
- Robertson SP, Lipp H, Bankier A. 1998. Zimmermann–Laband syndrome in an adult. Long-term follow-up of a patient with vascular and cardiac complications. *Am J Med Genet* 78:160–164.
- Sagai T, Masuya H, Tamura M, Shimizu K, Yada Y, Wakana S, Gondo Y, Noda T, Shiroishi T. 2004. Phylogenetic conservation of a limb-specific, cis-acting regulator of Sonic hedgehog (*Shh*). *Mamm Genome* 15:23–34.
- Schouten JP, McElgunn CJ, Waaijer R, Zwijnenburg D, Diepvens F, Pals G. 2002. Relative quantification of 40 nucleic acid sequences by multiplex ligation-dependent probe amplification. *Nucleic Acids Res* 30:57.
- Schwartz S, Zhang Z, Frazer KA, Smit A, Riemer C, Bouck J, Gibbs R, Hardison R, Miller W. 2000. PipMaker—a web server for aligning two genomic DNA sequences. *Genome Res* 10:577–586.
- Stefanova M, Atanassov D, Krastev T, Fuchs S, Kutsche K. 2003. Zimmermann–Laband syndrome associated with a balanced reciprocal translocation t(3;8)(p21.2;q24.3) in mother and daughter: Molecular cytogenetic characterization of the breakpoint regions. *Am J Med Genet Part A* 117A:289–294.
- Sutajova M, Neukirchen U, Meinecke P, Czeizel AE, Timar L, Solyom E, Gal A, Kutsche K. 2004. Disruption of the *PDGFB* gene in a 1;22 translocation patient does not cause Costello syndrome. *Genomics* 83:883–892.
- Van Buggenhout GJ, Brunner HG, Trommelen JC, Hamel BC. 1995. Zimmermann–Laband syndrome in a patient with severe mental retardation. *Genet Couns* 6:321–327.
- Woods CG, Stricker S, Seemann P, Stern R, Cox J, Sherridan E, Roberts E, Springell K, Scott S, Karbani G, Sharif SM, Toomes C, Bond J, Kumar D, Al-Gazali L, Mundlos S. 2006. Mutations in *WNT7A* cause a range of limb malformations, including Fuhrmann syndrome and Al-Awadi/Raas-Rothschild/Schinzel phocomelia syndrome. *Am J Hum Genet* 79:402–408.
- Yamaguchi TP, Bradley A, McMahon AP, Jones S. 1999. A *Wnt5a* pathway underlies outgrowth of multiple structures in the vertebrate embryo. *Development* 126:1211–1223.